Published in IET Science, Measurement and Technology
Received on 26th February 2011
doi: 10.1049/iet-smt.2011.0041

ISSN 1751-8822

Modification on a fast meshless method for electromagnetic field computations

H. Razmjoo M. Movahhedi A. Hakimi

Department of Electrical Engineering, Shahid Bahonar University of Kerman, Kerman, Iran
E-mail: movahhedi@ieee.org

Abstract: This study modifies and discusses the application of a complete meshless method based on Shepard approximation with an emphasis on the detailed description of this computational technique and its numerical implementations. A new weighting function would be suggested. The global shape function and its derivatives are built based only on the discretisation of the domain in nodes. To deal with the essential boundary condition problem, an alternative method has been proposed. The method is also capable of treating physical discontinuities present at interfaces between different matters. Application of proposed method for the electromagnetic field computation and verification of the obtained results using finite difference method and radial point interpolation method is also presented. The results demonstrate a good agreement between the proposed meshless method and other numerical techniques. So, an adequacy accuracy of this methodology can be concluded whereas the approximation functions have lower computational costs.

1 Introduction

Finite-element method (FEM) is a powerful method for modelling complex problems in applied electromagnetics. The mesh generation procedure is a necessary step for using the general FEM to solve partial differential equations (PDEs). However, the mesh generation can be tedious and time-consuming. In other words, for a given distribution of nodes, it is possible to obtain a mesh quickly, but it may also require several iterations, including manual interaction, to achieve an acceptable mesh.

The development of a method that does not need the mesh generation for complex structures is still very attractive. Over the last decade, a number of meshless or meshfree methods have been proposed [1]. Different authors have recently investigated the possibility of deriving numerical methods where meshes are unnecessary. The first efforts were reported by some finite-difference practitioners deriving finite-difference schemes in arbitrary irregular grids [2–5]. An alternative class of these methods called smooth particle hydrodynamics (SPH), depend only on a set of disordered points or particles and has enjoyed considerable popularity in computational physics [6]. Belytschko *et al.* have proposed an extension of the FEM which they call the element-free Galerkin (EFG) method [7]. Duarte and Oden [8] and Babuska *et al.* have formalised this type of approximation as a subclass of the so-called partition of unity methods (PUMs) [9, 10] and they propose meshless and enhanced finite-element procedures using hierarchical PU interpolations. A newcomer meshless method is the natural element method (NEM). This method is based on the natural neighbour concept to define the shape functions [11]. NEM has been used with a weak form by Sukumar *et al.* [12]. The point interpolation method (PIM) is a meshfree interpolation technique that was used by Liu and Gu [13] to construct shape functions using nodes distributed locally to formulate meshless weak-form methods. Different from the moving least square (MLS) approximation, PIM uses interpolations to construct shape functions that possess Kronecker delta function property. Two different types of PIM formulations using the polynomial basis [14] and the radial basis function (RBF), called radial point interpolation method (RPIM) [15–17], have been developed. In [18, 19], some recent developments of using RBFs in electromagnetic problems can be found. In [20], a special class of PUM is used and its efficiency in electrostatic problem, cartesian and polar coordinates, has been verified. The distinguished advantage of this method is in non-uniform node distribution domain which the shape functions are constructed according to nodes density.

All these methods have some weaknesses that usually make conventional meshless techniques inaccurate and/or high computational complexity methods. For example, in [21] authors have shown that the MLS approximation is not able to provide useful shape functions in every situation in electromagnetic problems or in [20] it is concluded that RPIM is not sure-footed in non-uniform node distributions.

This paper focuses on a great challenge in meshless methods, that is, shape function construction. According to the data-fitting algorithm and PUM, a complete approach for constructing shape functions would be proposed and its performance in electromagnetics problems in different situations would be investigated. A new weighting function is suggested so that shape function derivatives can be obtained easily in the closed forms (not numerically). Since there is no mesh information, the essential boundary

conditions can be forced without difficulty and interface conditions which are caused as a result of the physical discontinuities would be imposed in a new and efficient manner. It is simple to programme and in comparison with the most traditional schemes of the meshless methods is faster; however, its accuracy can be at the same level.

2 Approximation function and its derivatives

Most of conventional meshless methods need to compute the inversion of a matrix, which is usually an expensive process, to obtain the shape functions. In the proposed procedure introduced in the rest of the paper, there is no need to do that; and therefore shape functions can be constructed faster [22].

Typically, in a data-fitting process, a fitting algorithm produces a function F which is of the form $F(x) = \sum_i f_i N_i(x)$ where the values f_i are known data (e.g. function values, derivatives etc.). Known functions N_i are usually called shape functions.

One class of fitting algorithms is based on the so-called 'inverse distance weighted methods' whose ancestor is Shepard's method [23]. In the basic Shepard method, scattered data (x_i, f_i) are interpolated by a function as

$$F(x) = \frac{\sum_i f_i.w_i(x)}{\sum_i w_i(x)} \tag{1}$$

where the weights, that is $w_i(x)$, are typically chosen as decaying functions of the distance of x from the points x_i. The basic shape functions are thus as

$$N_i(x) = \frac{w_i(x)}{\sum_i w_i(x)} \tag{2}$$

and the global approximation of F takes the form

$$F(x) = \sum_i f_i.N_i(x) \tag{3}$$

Here, we propose a new shape function with continuity and partition of unity properties [13], which are essential provisions of any shape function, directly. This function is as follows [for one-dimensional (1D)]

$$N_i(x) = \frac{\exp(\alpha|x - x_i|)}{P(x)} \tag{4}$$

where, $P(x) = \sum_i \exp(\alpha|x - x_j|)$. In other words, the weights of the Shepard method in the proposed approach is as

$$w_i(x) = w(x - x_i) = \exp(\alpha|x - x_i|) \tag{5}$$

α is an independent positive coefficient that can change the overhang width of the shape function and its optimal setting increases the accuracy of the method. Unlike PUM, there is no need to use more than one unknown per each node to achieve acceptable accuracy [1].

Since some of the shape functions, arisen from conventional meshless methods, do not satisfy the Kronecker delta function property [13], imposition of the essential boundary conditions is another problem in these methods. Some authors have proposed the use of Lagrange multiplier and penalty method, among other techniques, to overcome this drawback [24]. In [25], authors proposed a mixed formulation that uses two different types of shape functions on the same problem domain. Another mixed formulation has been presented in [26] which combines Shepard's shape functions for inner nodes to reduce the computational time and RPIM shape functions for boundary nodes to impose the essential boundary conditions.

It is interesting to note that in the suggested shape function, by becoming smaller the overhang radius of the shape function using correct set of α, the value of the shape function in the other nodes would be close to zero. So, the boundary conditions will be imposed accurately with no trouble [27, 28]. For this reason, to construct the shape functions that correspond to boundary nodes (which lie on the Dirichlet boundaries), we can choose appropriate value for α to obtain the overhang radius of the function small enough. This manner makes possible it to impose essential boundary conditions, directly.

Another advantage of the proposed shape function, unlike the shape function introduced in [20], is that its derivatives can be obtained in closed forms, simply. For 1D, derivatives of this function can be presented as follows

$$\frac{\partial N_i(x)}{\partial x} = \alpha\left[-\text{sign}(x - x_i) + \frac{s_1}{s_0}\right].N_i(x) \tag{6}$$

$$\frac{\partial^2 N_i(x)}{\partial x^2} = 2\alpha\frac{\partial N_i(x)}{\partial x}.\frac{s_1}{s_0} \tag{7}$$

and so on, where

$$s_0 = P(x) = \sum_i w_i(x),\ s_1 = \sum_i \text{sign}(x - x_i).w_i(x) \tag{8}$$

The proposed shape function in 2D is as follows

$$N_i(x, y) = N(x - x_i, y - y_i) = \frac{\exp(\alpha_x|x - x_i| + \alpha_y|y - y_i|)}{P(x, y)} \tag{9}$$

(x_i, y_i) are coordinates of node i. Its derivatives would be obtained as

$$\frac{\partial N_i(x, y)}{\partial x} = \alpha_x\left[-\text{sign}(x - x_i) + \frac{s_{1x}}{s_0}\right].N_i(x, y) \tag{10}$$

$$\frac{\partial N_i(x, y)}{\partial y} = \alpha_y\left[-\text{sign}(y - y_i) + \frac{s_{1y}}{s_0}\right].N_i(x, y) \tag{11}$$

$$\frac{\partial^2 N_i(x, y)}{\partial x^2} = 2\alpha_x\frac{\partial N_i(x, y)}{\partial x}.\frac{s_{1x}}{s_0} \tag{12}$$

$$\frac{\partial^2 N_i(x, y)}{\partial y^2} = 2\alpha_y\frac{\partial N_i(x, y)}{\partial y}.\frac{s_{1y}}{s_0} \tag{13}$$

$$\frac{\partial^2 N_i(x, y)}{\partial x\partial y} = \alpha_x\frac{\partial N_i}{\partial y}.\frac{s_{1x}}{s_0} + \alpha_y\frac{\partial N_i}{\partial x}.\frac{s_{1y}}{s_0} + \alpha_x\alpha_y .\left[\text{sign}(x - x_i).\text{sign}(y - y_i) - \frac{s_{1xy}}{s_0}\right].N_i(x, y) \tag{14}$$

doi: 10.1049/iet-smt.2011.0041

and so on, where

$$
\begin{aligned}
s_0 &= P(x, y) = \sum_i w_i(x, y) \\
s_{1x} &= \sum_i \text{sign}(x - x_i).w_i(x, y) \\
s_{1y} &= \sum_i \text{sign}(y - y).w_i(x, y) \\
s_{1xy} &= \sum_i \text{sign}(x - x_i).\text{sign}(y - y_i).w_i(x, y)
\end{aligned} \tag{15}
$$

Moreover, the shape function and its derivatives, in 3D can be achieved, similarly. Here, a 2D example is presented to illustrate the properties of the proposed shape function and its derivatives created using 25 nodes in a rectangular domain with parameters $\alpha_x = 5/d_x$ and $\alpha_y = 5/d_y$. d_x and d_y are average nodal spacing in x and y directions, respectively. Figs. 1*a*–*d* show the proposed shape function and its derivatives related to one of the middle nodes on an uniform (5×5) node distribution. Also, Fig. 2 illustrates the shape functions of other two conventional meshless methods, that is, MLS approximation and thin plate spline radial point interpolation method (TPS-RPIM) [12]. As it is seen in Fig. 1*a* and Fig. 2, the general form of the proposed shape function is similar to some of the other shape functions obtained by conventional meshless methods; except that the function can be obtained directly with very low computational cost.

The proposed shape functions and their derivatives possess acceptable continuity to use them for solving electromagnetic problems by the meshless methods. Simplicity of the proposed function leads to fast obtaining of all shape functions and decrease the simulation time of the meshless method. Fig. 3 illustrates the consuming time for shape function construction in two methods, proposed method and RPIM approach. As it is seen, when the number of nodes, that is, $M(= N^2)$ increases, the RPIM method processing time increases, extremely. This is owing to the computation of a $(M \times M)$ matrix inversion for its shape functions' construction. However, in the introduced method when the shape functions are constructed directly, there is no need to

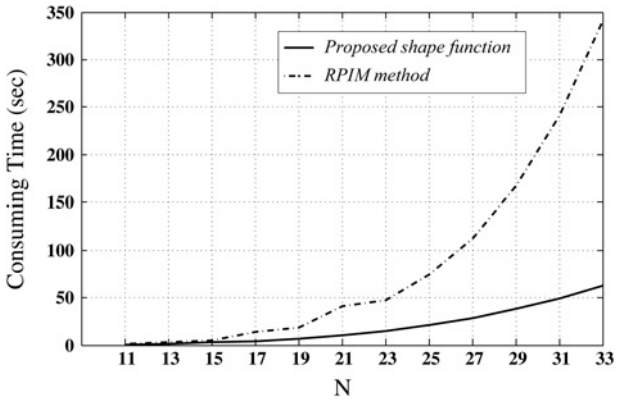

Fig. 3 *Consuming time to construct the shape functions in proposed direct and RPIM methods for different number of nodes*

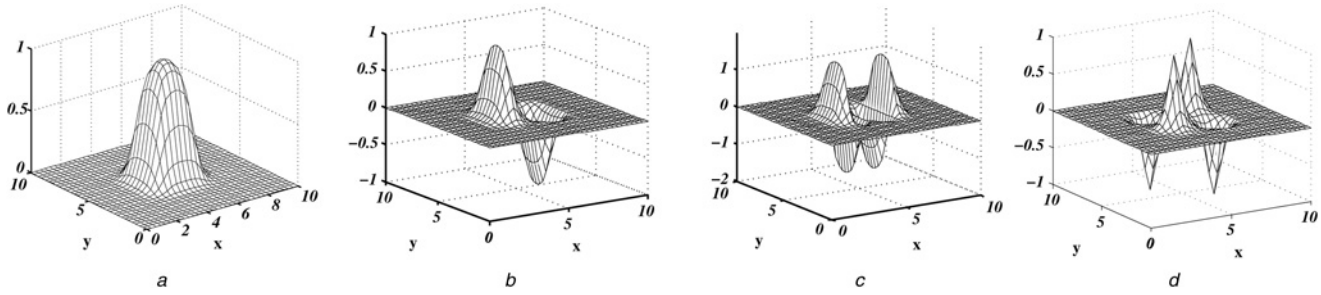

Fig. 1 *Proposed shape function and its derivatives on a (5×5) uniform node distribution for one of the middle nodes*

a Shape function $[N(x, y)]$
b $[\partial N(x, y)]/(\partial x)$
c $[\partial^2 N(x, y)]/(\partial x^2)$
d $[\partial^2 N(x, y)]/(\partial x \partial y)$

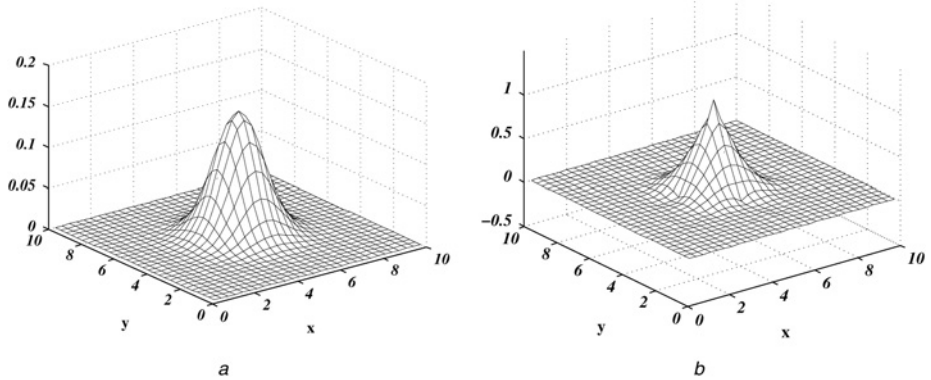

Fig. 2 *Shape functions which are constructed by two other methods*

a MLS shape function
b TPS-RPIM shape function

compute this matrix inversion. So, in the RPIM method, by increasing the number of nodes when the dimension of the resulted matrix is enlarged, the load of calculations would increase, extremely.

3 Meshless formulation

According to the formulation procedures, meshless methods fall into two categories, meshless methods based on collocation or strong form and weak forms [13, 29, 30]. In meshless weak-form methods, the governing PDEs with derivative boundary conditions are first transformed to a set of so-called weak-form integral equations. In almost all electromagnetic problems, the boundary-value problems under consideration are defined by a second-order differential equation as [32]

$$-\frac{\partial}{\partial x}\left(\beta_x\frac{\partial\phi}{\partial x}\right)-\frac{\partial}{\partial y}\left(\beta_y\frac{\partial\phi}{\partial y}\right)-\frac{\partial}{\partial z}\left(\beta_z\frac{\partial\phi}{\partial z}\right)+\beta\phi=f \quad \text{in } \Omega \tag{16}$$

where ϕ is the unknown field function, β_x, β_y, β_z and β are known parameters or functions associated with the physical properties of the solution domain and f is a known source or excitation function. All types of boundary conditions could be expressed as essential (Dirichlet) boundary condition

$$\phi=p \quad \text{on } \Gamma_1 \tag{17}$$

or boundary condition of the third kind as

$$\left(\beta_x\frac{\partial\phi}{\partial x}\hat{a}_x+\beta_y\frac{\partial\phi}{\partial y}\hat{a}_y+\beta_z\frac{\partial\phi}{\partial z}\hat{a}_z\right).\hat{n}+\gamma\phi=q \quad \text{on } \Gamma_2 \tag{18}$$

where $\Gamma(=\Gamma_1+\Gamma_2)$ denotes the contour or enclosing of area Ω (problem domain), $\hat{n}$ is its outward normal unit vector and γ, p and q are known parameters. To use the variational method to formulate the meshless method, we need first to establish the required variational principle. For the problem above, it can be shown that its solution can be obtained by solving the equivalent variational problem defined by

$$\begin{cases}\delta F(\phi)=0\\ \phi=p \qquad \text{on } \Gamma_1\end{cases} \tag{19}$$

where

$$F(\phi)=\frac{1}{2}\iiint_\Omega\left[\beta_x\left(\frac{\partial\phi}{\partial x}\right)^2+\beta_y\left(\frac{\partial\phi}{\partial y}\right)^2+\beta_z\left(\frac{\partial\phi}{\partial z}\right)^2+\beta\phi^2\right]\mathrm{d}\Omega + \int_{\Gamma_2}\left(\frac{\gamma}{2}\phi^2-q\phi\right)\mathrm{d}\Gamma-\iiint_\Omega f\phi\ \mathrm{d}\Omega \tag{20}$$

It means that by minimising (20) and enforcing essential boundary condition, the unknown field function can be obtained. The field function $[\phi(x)]$ would be approximated in the meshless method as

$$\tilde{\phi}(\boldsymbol{x})=\sum_{i=1}^{N}N_i(\boldsymbol{x}).a_i \tag{21}$$

where N_i are the shape functions, a_i are the unknown coefficients which must be obtained and N is the number of nodes. By substituting (21) into (20) and taking the derivative of F with respect to a_i, we obtain

$$\frac{\partial F}{\partial a_i}=\sum_{j=1}^{N}a_j\iiint_\Omega\left(\beta_x\frac{\partial N_i}{\partial x}\frac{\partial N_j}{\partial x}+\beta_y\frac{\partial N_i}{\partial y}\frac{\partial N_j}{\partial y}+\beta_z\frac{\partial N_i}{\partial z}\frac{\partial N_j}{\partial z}+\beta N_iN_j\right)\mathrm{d}\Omega-\iiint_\Omega fN_i\mathrm{d}\Omega=0,\quad i=1,2,\ldots,N \tag{22}$$

Note that if the shape functions satisfy the Kronecker delta function property, coefficients a_i would be equal to the value of unknown field ϕ at related nodes.

One of the complications in meshless methods is that computing these appeared integrals in above relations over the entire problem domain is a time-consuming step. As Fig. 1 shows, it is evident that the proposed shape function and its derivatives have an influence domain where their values are considerable. Out of this domain in a recognisable distance from related node, the shape function and its derivatives have very small values, nearly close to zero. By finding out α in (4) or α_x and α_y in (9), damping ratio of the shape function and also this distance can be evaluated accurately. So, we can employ a relaxed weak form with integration over a small local quadrature domain, that is, influence domain. However, in the other schemes of the meshless methods, it is very difficult to evaluate this distance accurately or in some of them, like MQ-RPIM, the shape function has zero value in a far distance from related node. Therefore by using the proposed shape function in a meshless method, a lot of time can be saved in this step too.

4 Discontinuity consideration

The strongest emphasis in the construction of meshless approximations has so far been placed on simple domains, such as rectangular and simply connected bodies, with constant or smoothly varying parameters in the governing equations. However, many practical problems involve multiply connected domains and various discontinuities in the solution. The great hardship in dealing with the discontinue boundary revolves around the definition of the corresponding weight functions near the discontinuity. If the influence domain of the shape function or approximation function is completely cut by a discontinuity, which comes from multiply connected domain, the approximation function will be discontinued across the edge. However, high-order continuity property of traditional meshless shape functions provides a smooth solution with smooth derivatives. So, the treatment of those domains of influence can be crucial to the accuracy of the method [1, 31].

In meshless methods, the introduction of discontinuities also requires special consideration. The conventional techniques would made weight functions discontinuous and the discontinuity of weight functions determines the discontinuity of the shape functions.

In this paper, to create discontinuities in proposed weight function, a simple and efficient approach is suggested. To do that, a function which related to discontinuous parameter is multiplied by those weight functions that have non-zero values at discontinuous edge. For example, if a line of discontinuity is considered, the domain of influence of a

doi: 10.1049/iet-smt.2011.0041

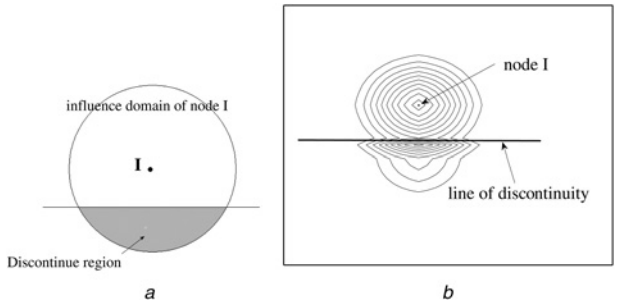

Fig. 4 *Proposed treatment for discontinuity*

a Domain of influence of a node (I) adjacent to a line of discontinuity
b Contour plots of the shape function for node I adjacent to a line of discontinuity

generic node I in the vicinity of a discontinuity takes the shape shown in Fig. 4*a*. Points in the shaded region of the original domain of influence would be multiplied by the discontinuous function. This function can be related to a discontinuous parameter (e.g. μ_r or ε_r). For instants, we suggest this function to be

$$G(\zeta) = \begin{cases} 1/(1+\zeta^p) & \text{in discontinuous region} \\ 1 & \text{other regions} \end{cases} \tag{23}$$

where ζ is the discontinuous parameter and p is a constant. It is important to note that, to have better results, the discontinuous function must be chosen according to the discontinuity condition. A consequence of this approach is that a discontinuity is introduced into weight function and shape function wherever the domain of influence is cut by a line of discontinuity. Contour plots for the shape function of node I is shown in Fig. 4*b*. It should be mentioned that this discontinuity do not lead to failure of convergence. In the next section, it will be shown that the resulting approximations can lead to a convergent solution.

5 Numerical experiments

To validate and demonstrate the advantages and shortcomings of the proposed method, three examples have been presented. Unfortunately, there are no exact solutions to obtain electromagnetic fields in these geometries; so we use the finite-difference method (FDM), which is the most famous computational method, as a criterion response. At first, behaviour of the proposed method in a magnetostatic problem is assessed. This is done by examining the distortion of the magnetic field owing to the interface between the air and a magnetic material bar (with $\mu_r = 1000$). The problem geometry, which is a rectangular box in xy-plane ($0 < x < 0.1$ m and $0 < y < 0.1$ m), and used node distribution for applying proposed meshless method and FDM are illustrated in Fig. 5*a*. The magnetic vector potential $\boldsymbol{A}$ is obtained by solving the static vector wave equation for magnetic potential as

$$\nabla \times \left(\frac{1}{\mu_r}\nabla \times \boldsymbol{A}\right) = \mu_0 \boldsymbol{J} \tag{24}$$

Then, magnetic flux density can be calculated from $\boldsymbol{A}$ as $\boldsymbol{B} = \nabla \times \boldsymbol{A}$. In this problem, boundary conditions on the outer bounds are $A_z = 0$ at $x = 0$, $A_z = 1$ Wb/m at $x = 0.1$ m, and $\partial A_z/\partial n = 0$ at $y = 0$ and $y = 0.1$ m. In this example, there is a high level of discontinuity in magnetic field but vector potential $\boldsymbol{A}$ has a continual change. To solve it using the meshless method based on the introduced shape function, it was found that $\alpha_x = \alpha_y = 3/d_c$ led to good results in the analysis of 2D magnetostatic problems, where d_c is nodal spacing in each direction. Fig. 5*b* shows the magnetic flux density, $\boldsymbol{B}$, observed along a straight line of 16 nodes crossing the materials interface at $y = 0.06$ m with $x = 0 \rightarrow 0.1$ m. An illustrative comparison between the results of two methods, that is, proposed meshless method and FDM, is shown in this figure.

The second example concentrates at the wave equation. In this example we attempt to solve an electromagnetic problem that covers some challenges of the computational electromagnetic. Problem is a partially filled parallel-plate waveguide, the geometry of which has been illustrated in Fig. 6*a*, where a guided wave is propagating from left to right. Owing to the existence of a dielectric rod, a partition of the power carried by the incident wave can pass and continue to propagate along the waveguide. Another partition of the power will be reflected. To study this problem mathematically, let us assume that the waveguide is operating at a low-enough frequency so that only the low-dominant mode, that is, TE_z mode, can propagate without attenuation. On the left side sufficiently away from the discontinuity, the wave can be expressed as a summation of the incident and reflected waves, that is

$$H_z = H_z^{\text{inc}} + H_z^{\text{ref}} = H_0 e^{-jk_0 x} + RH_0 e^{jk_0 x} \tag{25}$$

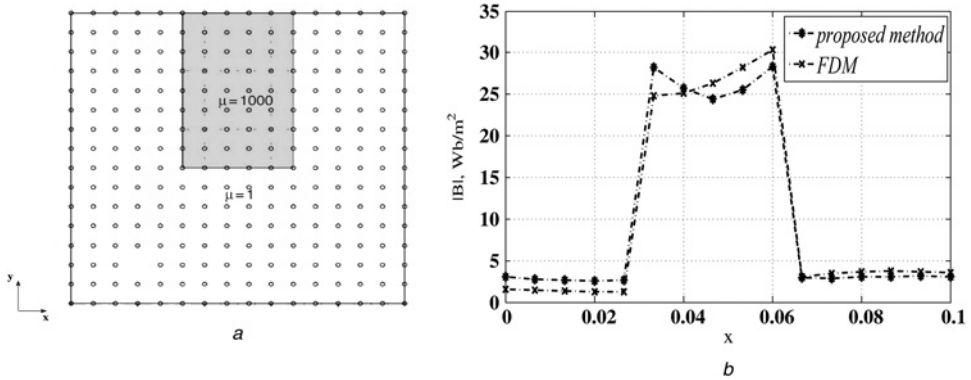

Fig. 5 *Magnetostatic problem*

a Diagram of material interface problem; circles represent nodal distribution
b Magnetic flux density computed at $y = 0.06$ m from $x = 0 \rightarrow 0.1$ m

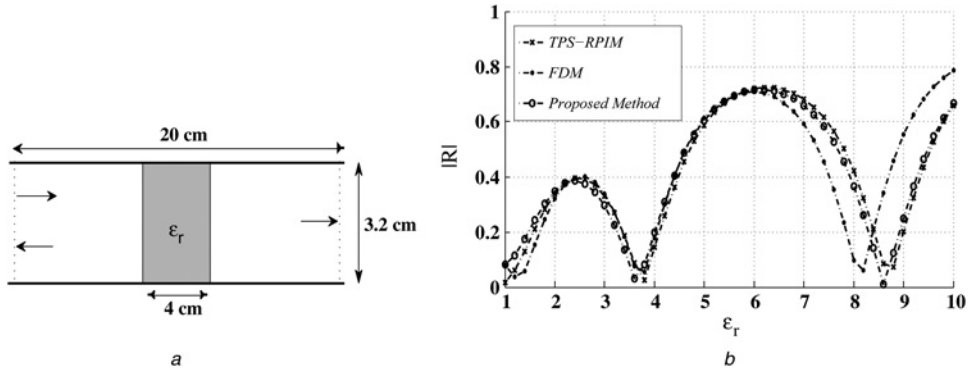

Fig. 6 *Parallel-plate waveguide with dielectric material rod*

a Dielectric rod inserted in a parallel-plate waveguide
b Reflection coefficient as a function of the rod dielectric constant computed by three methods

where H_0 is a constant, R denotes the reflection coefficient and k_0 is the propagation constant. The problem then becomes the determination of R. It can only be determined by solving the governing differential equation, that is, wave equation as

$$\frac{\partial}{\partial x}\left(\frac{1}{\varepsilon_r}.\frac{\partial H_z}{\partial x}\right)+\frac{\partial}{\partial y}\left(\frac{1}{\varepsilon_r}.\frac{\partial H_z}{\partial y}\right)+\mathrm{j}k_0^2\mu_r H_z=0 \tag{26}$$

together with the boundary condition at the waveguide walls as

$$\frac{\partial H_z}{\partial n}=0 \tag{27}$$

In this problem, H_z is considered as the tangential component of magnetic field intensity at interfaces. Owing to the continuity condition of the magnetic field tangential components on the interface of two different dielectrics, H_z does not change, abruptly. Therefore there is no need to create discontinuities in the shape function of the meshless method. The currently infinite domain must be reduced or truncated into a finite domain. To truncate the solution domain, two artificial boundaries at each side are introduced. With regard to the left-side boundary, if the boundary is sufficiently far from the discontinuity, the field can be approximated by (25) and thus we have

$$\begin{aligned}\frac{\partial H_z}{\partial x}&\simeq -\mathrm{j}k_0H_0\mathrm{e}^{-\mathrm{j}k_0x}+\mathrm{j}k_0H_0R\mathrm{e}^{\mathrm{j}k_0x}\\&=\mathrm{j}k_0H_z-2\mathrm{j}k_0H_0\mathrm{e}^{-\mathrm{j}k_0x}\end{aligned} \tag{28}$$

This can be used as the boundary condition at the left boundary. Similarly, we obtain the approximation boundary condition at the right boundary as

$$\frac{\partial H_z}{\partial x}\simeq -\mathrm{j}k_0H_z \tag{29}$$

In this example, we choose $\alpha_x=\alpha_y=2/d_c$ for inner nodes and $\alpha_x=\alpha_y=4/d_c$ for boundary nodes. Fig. 6*b* gives the results for the reflection coefficient as a function of the rod dielectric constant. Also in this figure, a comparison of the numerical results obtained with other conventional methods, that is, FDM and TPS-RPIM method [13], in the same node distribution is illustrated. As seen in this figure, by correct selection of the shape parameter, that is, α, the proposed meshless method based on the new shape function, achieves the same level of accuracy, whereas the method can save a part of the computational time.

Finally, to evaluate this meshless method in an electromagnetic problem with discontinuous domain, we suggest another parallel-plate waveguide, as seen in Fig. 7, which is partially filled with a magnetic material. In this problem, to obtain TE_z mode solution, the wave equation for z component of the magnetic field intensity, that is, (26), along with the boundary conditions at the waveguide walls, that is, (27), and interface Γ must be solved. According to the continuity condition of the magnetic flux density normal components on the interface of two materials, that is, $\mu^+H_n^+=\mu^-H_n^-$, and since H_z is the normal component on boundary Γ, H_z must be subjected to sudden changes on this boundary. Therefore in applying the meshless method to this problem, the shape functions must be discontinuous at this interface. To do this, as mentioned in Section 4, function $G(\zeta)$ is multiplied by the shape functions related to this boundary nodes. In this case ζ, which is related to discontinuous parameter, is μ_r and we set $p=1.6$ in (27). Also to have a better solution, the boundary condition can be directly forced on this edge nodes using the strong form. By utilising these two approaches, the boundary conditions would be imposed, accurately.

Figs. 8*a* and *b* show the real part of H_z observed along a straight line of crossing the material and the equipotential lines of real part of H_z obtained by the proposed meshless method where $\mu_r=4$, respectively. Abrupt change of solution is clearly observable in these figures.

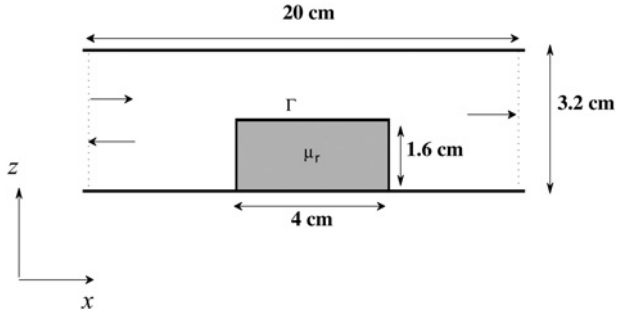

Fig. 7 *Magnetic material rod inserted in a parallel-plate waveguide*

doi: 10.1049/iet-smt.2011.0041

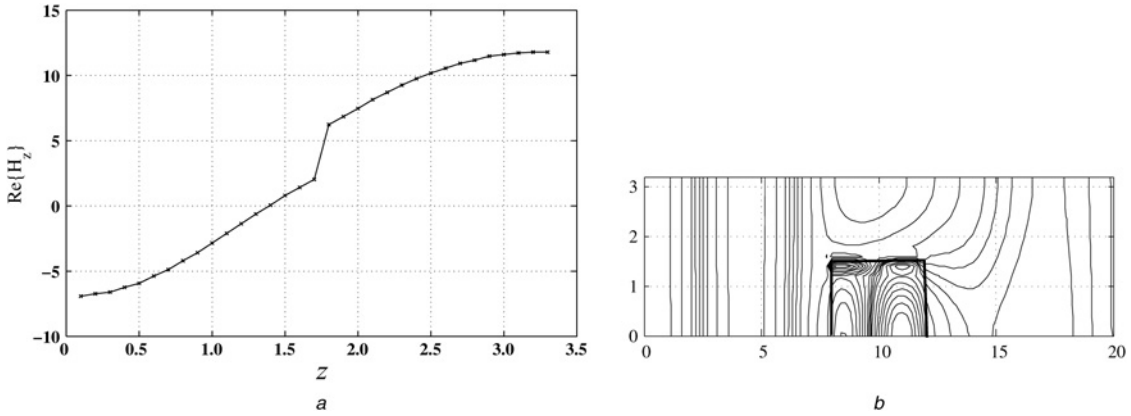

Fig. 8 *Field in the parallel plate waveguide with a magnetic material rod*

a Real part of H_z observed along a straight line of crossing the material at $x = 10$ cm
b Equipotential lines of real part of H_z

6 Conclusion

In this paper, we have presented a fast-modified meshless method in detail to be efficient for electromagnetic fields computation. In order to do so, first we introduced a new weighting function which formed simply and the corresponding shape function derivatives can be calculated easily in closed form. Also these closed-form formulas for them were presented. In addition, to impose the essential boundary condition in electromagnetic problems, an efficient technique was proposed. It was shown that, in the boundary nodes, by becoming smaller the overhang radius of the shape functions using correct choice of the function shape parameter, the essential boundary condition would be imposed accurately with no trouble. Moreover, to have a discontinuous shape function in problems with discontinuity conditions, a function which is related to discontinuous parameter, is multiplied by the weighting functions which have non-zero values at discontinuous edge. This discontinuous function must be chosen according to the discontinuity condition. Finally, several examples have verified the accuracy and convergence characteristics of the proposed method. These examples illustrated that, by these modifications, the proposed Shepard function approximations can reach acceptable accuracy in computational electromagnetic while they can save considerable computational time.

7 Acknowledgment

This work was supported in part by the Education and Research Institute for ICT of Iran (ERICT).

8 References

1 Belytschko, T., Krongauz, Y., Organ, D., Fleming, M., Krysl, P.: 'Meshless method: an overview and recent developments', *Comput. Meth. Appl. Mech. Eng.*, 1996, **139**, pp. 3–47
2 Forsythe, G.E., Wasow, W.R.: 'Finite difference method for partial differential equations' (Wiley, New York, 1960)
3 Perrone, N., Kao, R.: 'A general finite difference method for arbitrary mesh', *Comput. Struct.*, 1975, **5**, pp. 45–57
4 Liszka, T., Orkisz, J.: 'The finite difference method at arbitrary irregular grids and its application in applied mechanics', *Comput. Struct.*, 1980, **11**, pp. 83–95
5 Liszka, T.: 'An interpolation method for an irregular set of nodes', *Int. J. Numer. Methods Eng.*, 1994, **37**, pp. 229–256
6 Liu, G.R., Liu, M.B.: 'Smoothed particle hydrodynamics' (World Scientific Publishing Co. Ltd., 2003)
7 Belytschko, T., Lu, Y.Y., Gu, L.: 'Element-free Galerkin method', *Int. J. Numer. Methods Eng.*, 1994, **37**, pp. 229–256
8 Duarte, C.A., Oden, J.T.: 'Hp clouds – a meshless method to solve boundary value problem', Texas Institue for Computational and Applied Mathematics, University of Texas at Austin, Technical Report 95-05, 1995
9 Melenk, J.M., Babuska, I.: 'The partition of unity finite element method: basic theory and applicathions', *Comput. Meth. Appl. Mech. Eng.*, 1996, **139**, pp. 289–314
10 Babuska, I., Melenk, J.M.: 'The partition of unity method', *Int. J. Numer. Methods Eng.*, 1997, **40**, pp. 727–758
11 Sibson, R.: 'A vector identity for the dirichlet tessellation', *Math. Proc. Camb. Philos. Soc.*, 1980, **87**, (1), pp. 151–155
12 Sukumar, N., Moran, B., Semenov, A., Belikov, V.: 'Natural neighbour Galerkin methods', *Int. J. Numer. Methods Eng.*, 2001, **50**, pp. 1–27
13 Liu, G.R., Gu, Y.T.: 'An introduction to meshfree methods and their programming' (Springer, 2005)
14 Liu, G.R., Gu, Y.T.: 'A point interpolation method for two-dimensional solids', *Int. J. Numer. Methods Eng.*, 2001, **50**, pp. 937–951
15 Viana, S.A., Rodger, D., Lai, H.C.: 'Meshless local Petrov–Galerkin method with radial basis functions applied to electromagnetics', *IEE Proc. Sci. Meas. Technol.*, 2004, **151**, (6), pp. 449–451
16 Guimaraes, F.G., Saldanha, R.R., Mesquita, R.C., Lowther, D.A., Ramirez, J.A.: 'A meshless method for electromagnetic field computation based on the multi-quadric technique', *IEEE Trans. Magn.*, 2007, **43**, (4), pp. 1281–1284
17 Lai, S.J., Wang, B.Z., Duan, Y.: 'Meshless radial basis function method for transient electromagnetic computations', *IEEE Trans. Magn.*, 2008, **44**, (10), pp. 2288–2295
18 Yang, G., Zhang, Y., Lei, G., *et al.*: 'A novel superposition RBF collocation method to solve moving conductor eddy current problems', *IEEE Trans. Magn.*, 2009, **45**, (10), pp. 3977–3980
19 Kanthamani, S., Vahini, N.S., Raju, S., Abhaikumar, V.: 'Quasi-static modelling of carbon nanotube interconnects for gigahertz applications', *IET Micro Nano Lett.*, 2010, **5**, (5), pp. 328–332
20 Razmjoo, H., Movahhedi, M., Hakimi, A.: 'An efficient meshless method based on a new shape function', *Int. J. Numer. Model., Electron. Netw. Devices Fileds*, 2010, **23**, (6), pp. 503–521
21 Nicomedes, W.L., Mesquita, R.C., Moreira, F.J.d.: '2-D scattering integral field equation solution through an IMLS meshless-based approach', *IEEE Trans. Magn.*, 2010, **46**, (8), pp. 2783–2786
22 Razmjoo, H., Movahhedi, M., Hakimi, A.: 'Improved meshless method using direct shape function for computational electromagnetics'. Proc. Asia-Pacific Microwave Conf. (APMC 2010), Yokohama, Japan, December 2010
23 Shephard, D.: 'A two-dimensional function for irregularly spaced data'. AMC National Conf., 1968, pp. 517–524
24 Liu, G.R.: 'Mesh free methods: moving beyond the finite element method' (CRC Press, Boca Raton, FL, 2002)
25 Fonseca, A.R., Viana, S.A., Silva, E.J., Mesquita, R.C.: 'Imposing boundary conditions in the meshless local Petrov–Galerkin method', *IET Sci. Meas. Technol.*, 2008, **6**, (2), pp. 387–394
26 Fonseca, A.R., Corrêa, B.C., Silva, E.J., Mesquita, R.C.: 'Improving the mixed formulation for meshless local Petrov–Galerkin method', *IEEE Trans. Magn.*, 2010, **46**, (8), pp. 2907–2910

27 Hkrault, C., Markcha, Y.: 'Boundary and interface conditions in meshless methods', *IEEE Trans. Magn.*, 1999, **35**, (3), pp. 1450–1453
28 Fonseca, A.R., Viana, S.A., Silva, E.J., Mesquita, R.C.: 'Imposing boundary conditions in the meshless local Petrov–Galerkin method', *IET Sci. Meas. Technol.*, 2008, **2**, (6), pp. 387–394
29 Kansa, E.J.: 'Multiquadrics – a scattered data approximation scheme with applications to computational fluid dynamics', *Comput. Math. Appl.*, 1990, **19**, pp. 127–145
30 Liu, X., Liu, G.R., Tai, K., Gu, Y.T., Lam, K.Y.: 'Polynomial point interpolation collocation method for the solution of partial differential equations', *Eng. Anal. Bound. Elem.*, 2006, **30**, (7), pp. 598–609
31 Jin, J.M.: 'The finite element method in electromagnetics' (John Wiley & Sons Ltd., 2002)
32 Organ, D., Fleming, M., Terry, T., Belytschko, T.: 'Continuous meshless approximation for nonconvex bodies by diffraction and transparency', *Comput. Mech.*, 1996, **18**, (3), pp. 225–235

doi: 10.1049/iet-smt.2011.0041